Enhancement of Sensing Range and Stability of Ultrasensitive Crack-based Strain Sensor Using Atomized Liquid Metal

Jinwon Jeong, *Graduate Student Member, IEEE*, Arkadeep Mitra, *Graduate Student Member, IEEE*, and Jeong Bong (JB) Lee, *Senior Member, IEEE*

***Abstract*—Biomimetic crack-based sensors are known for their ultrahigh sensitivity in strain sensing with gauge factors of ~2,000, but sensing range is very limited (~2%). We report a method of enhancing sensing range and stability of ultrasensitive crack-based sensor using atomized liquid metal droplets. A crack-based sensor was fabricated by depositing chromium/gold (0.9 nm/20 nm) bilayer on plasma-treated PDMS with an additional step of stretching the sensor to create myriads of cracks on metal film. After the formation of a conventional crack-based strain sensor, gallium-based liquid metal was sprayed over the sensor surface to randomly deposit atomized liquid metal droplets. Optical images of the crack-based sensor under applied strain showed the atomized liquid metal droplets act as stretchable conductive bridges between cracks in the strain sensor. By using randomly dispersed atomized liquid metal droplets, the crack-based sensor showed higher sensitivity (R/R_0 of ~238) and gauge factor of ~2,238 compared to the crack-based sensor without liquid metal. The sensing range of the crack-based sensor was enhanced from 2.283% to 10.675% with the aid of atomized liquid metal droplets. Flexibility of the liquid metal-aided crack-based sensor was also verified through repetitive testing of stretching, bending, and twisting.**

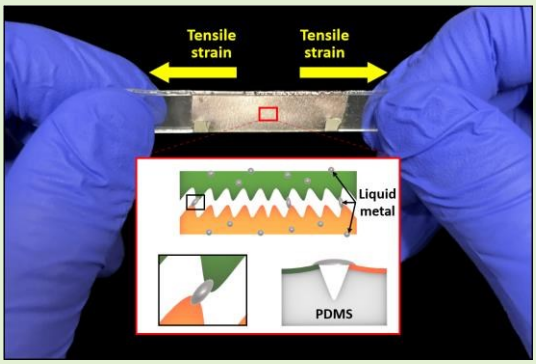

***Index Terms*—gallium, liquid metal, crack, strain, sensor**

I. Introduction

Wearable health devices such as electronic skin [1], biofluidic system [2], and drug delivery [3] have been studied for diagnosis of various diseases. Continuous and real-time monitoring of various health data including electrocardiogram (ECG) [4], sweat [5], and body temperature [6] have been demonstrated. Flexible wearable strain sensors also play a key role in wearable health monitoring devices and were widely used for monitoring human-motion detection [7, 8], bone loss [9, 10], blood pressure monitoring [11, 12], among others. With the flexible characteristic of material for sensors used in wearable devices, sensitivity of wearable sensor is one of the most important factors to achieve the fast recognition of bio-signals from a human body with high accuracy [13]. Numerous efforts have been devoted to the enhancement of sensitivity with fast response time and superior precision in wearable sensors by employing various novel materials such as carbon nanotubes (CNTs) [14-16], nanoparticles [17, 18], and carbon composites [19] or the optimization of the sensor design by using biomimetic receptors [20].

One of the most pioneering works in strain sensing in the recent years is a crack-based strain sensor inspired by the sensory system of a spider [21]. The approach in strain sensing in the crack-based strain sensor is markedly different from conventional strain sensors as the bio-inspired crack-based sensor utilizes an array of nanoscale cracks in platinum (Pt) deposited on polyurethane acrylate (PUA) showing ultrahigh gauge factor (GF) of ~2,000 at a strain of ~2%, a quantum leap of sensitivity enhancement in strain sensing. Numerous follow-up researches have been done and the sensitivity of the crack-based sensor has been improved even further with a gauge factor of ~16,000 through a precise modification of crack geometry especially in the depth of the cracks [22]. While the sensitivity is exceptionally high, the crack-based strain sensor is not without a disadvantage. One of the critical issues of the crack-based strain sensor in practical applications is its limited sensing range. Most crack-based sensors show sensing range only up to 2% of external strain as the sensor completely disconnects and does not function beyond the strain greater

This work was supported in part by the United States National Science Foundation grant NSF ECCS–1908779. An earlier version of this paper was presented at the 2022 *IEEE Sensors Conference* and was published in its Proceedings.

Jinwon Jeong is with the Department of Electrical and Computer Engineering, The University of Texas at Dallas, Dallas, TX 75080 USA (e-mail: jxj200042@utdallas.edu).

Arkadeep Mitra is with the Department of Electrical and Computer Engineering, The University of Texas at Dallas, Dallas, TX 75080 USA (e-mail: axm179431@utdallas.edu).

Jeong Bong (JB) Lee is with the Department of Electrical and Computer Engineering, The University of Texas at Dallas, Dallas, TX 75080 USA (e-mail: jblee@utdallas.edu).

than ~2% [23].

Gallium-based alloys such as Galinstan (a ternary alloy of gallium, indium, and tin) and EGaIn (an eutectic binary alloy of gallium and indium) are in liquid phase and metallic at around room temperature, having characteristics of liquid and metal together as they show infinite deformability and high electrical/thermal conductivity with biocompatibility [24-26]. When gallium-based liquid metal alloys are exposed to ambient air environment, they are instantly oxidized and a thin layer (0.5 ~ 3 nm) of gallium oxide (Ga_2O or Ga_2O_3) skin is formed. Such surface oxide layer makes the gallium-based liquid metal alloys adhere to almost any surfaces [27, 28]. Recently, gallium-based liquid metal has been used for a nacre-inspired wearable strain sensor which consists of a biphasic pattern of liquid metal with Cr/Cu underlayer as bricks and strain-sensitive silver film as mortar [29]. This unique wearable strain sensor demonstrated an overall gauge factor of 543 with a substantially extended sensing range up to 86.3%.

In this paper, we propose a simple yet powerful method of enhancement of the sensing range and stability of the crack-based sensor using randomly dispersed atomized gallium-based liquid metal droplets over the crack-based strain sensor. The instant surface oxidation of the gallium-based liquid metal makes the liquid metal droplets stick on the surface of the crack-based strain sensor and act as deformable conductive bridges between the cracks of the strain sensor, resulting in an increase of sensing range while maintaining the high sensitivity.

II. Principle And Fabrication

A. Principle

Figure 1 shows schematic diagrams why a crack-based sensor possesses ultrahigh gauge factor (e.g., ~2,000) which cannot be achieved by conventional strain sensors. Figure 1-a shows the initial state of the crack-based strain sensor before external mechanical strain is applied. Although there are cracks, resistance of the strain sensor (R_{eqi}) without an applied external axial loading is by one resistor with a large cross-sectional area since all cracks are connected. When a mechanical loading is applied to the crack-based sensor in the axial direction, the gap between cracked metal films starts to widen and it will be disconnected after a certain axial loading. However, the sensor is not immediately disconnected because transverse strain pushes the sensor on the side direction and have the numerous cracks in contact with substantially reduced contact area (Figure 1-b). Now, instead of one resistor, an array of countless parallelly-connected resistors with smaller cross section areas are formed. The contact area of the parallelly-connected resistors becomes smaller with increased axial loading, resulting in drastic increase in overall resistance. This in turn result in ultrahigh gauge factor which is not achievable with one resistor. While this sensing principle gives ultrahigh sensitivity (gauge factor of ~2,000), the sensor has a limited sensing range as the transverse strain effect can only go until an axial loading reaches ~2%. Axial loading beyond this limit makes the cracks permanently disconnected and the sensor no longer works.

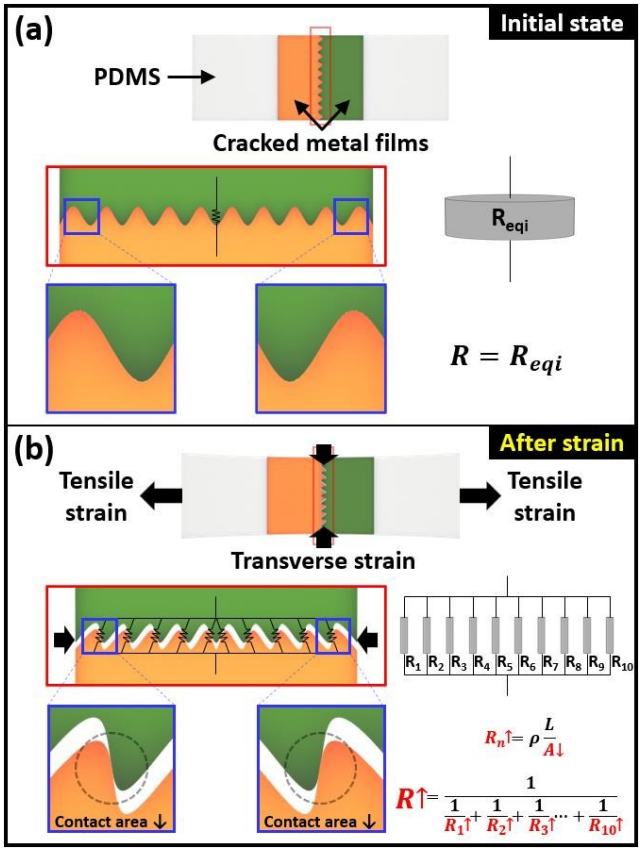

Fig. 1. Schematic diagrams of a principle of a ultrahigh sensitivity crack-based strain sensor: (a) initial state without any strain; (b) after applying external mechanical strain – showing the effect of the transverse strain.

In order to increase sening range of a crack-bassed strain sensor, we envisioned using atomized liquid metal droplet as stretchable conductive bridges between cracks. Figure 2 shows conceptual schematic diagrams of the crack-based sensor without liquid metal (Figure 2-a) compared to the randomly dispersed liquid metal droplets decorated crack-based sensor (Figure 2-b). The strain senor is designed to have a bilayer metal films (chromium/gold) on polydimethylsiloxane (PDMS) in which cracks are formed on the metal films. The bilayer metal films crack-based sensor is then spray-coated with atomized liquid metal droplets.

Without axial tensile strain (ε = 0 %), cracks are all connected showing one resistance (R_{eqi}) with a large cross section area (Figure 2-a1 and 2-b1) making no difference between the sensor without liquid metal and the sensor with liquid metal regardless of the presence of the atomized liquid metal droplets on the surface of the crack-based sensor. When a tensile strain is applied to the crack-based sensors with/without atomized liquid metal droplets, the cracks start to get widen, but because of the combination with the tensile and transverse strain, countless parallely-connected resistors with very small cross section areas form. As the tensile strain in the axial direction reaches ~2%, the crack-based sensor without liquid metal shows the highest sensitivity (Figure 2-a2), a gauge factor of ~2,000. When the applied tensile strain exceeds ~2%, the crack-based sensor without liquid metal cannot function as a sensor anymore because the metal film is completely

disconnected (Figure 2-a3) [21].

In the case of the crack-based sensor decorated with atomized liquid metal droplets, up to ~2% of axial strain, sensitivity is slightly lower than that of the crack-based sensor without liquid metal since the resistance is affected by the conductance of additional liquid metal droplets linked between cracked metal films (Figure 2-b2). When the applied tensile strain exceeds ~2 %, some of the randomly dispersed atomized liquid metal droplets sitting on the cracks start to act as extendable metallic bridges between edges of the cracks which prevents complete electrical disconnection of the crack-based sensor. Since not all of the parallely connected crack resistors are disconnected, sensing range is greatly increased while maintaining high sensitivity (Figure 2-b3). When the axial strain is continually increased, eventually all of the liquid metal droplet connected cracks will also be disconnected and the sensor cannot function any further.

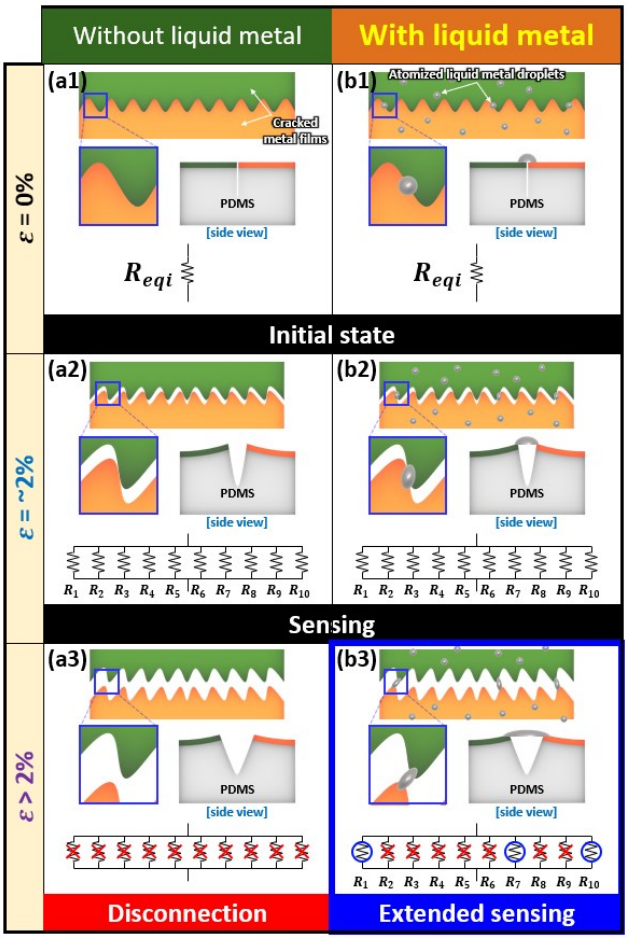

Fig. 2. Conceptual schematic diagrams of principle of the crack-based sensors. Countless parallelly connected resistors due to transverse strain results in greatly enhanced gauge factor: (a) crack-based sensor without liquid metal showing narrow sensing range up to ~2 % strain; (b) crack-based sensor with liquid metal showing extended sensing range due to deformable liquid metal bridges.

B. Fabrication

Figure 3 shows schematic diagrams of the fabrication sequence of an ultrasensitive crack-based sensor decorated with randomly dispersed atomized liquid metal droplets. Fabrication was started with a formation of a rectangular-shape PDMS as a body of the crack-based sensor with width of 10 mm, length of 60 mm, and thickness of 1 mm. Sylgard 184 (Dow Chemical Company, Midland, MI) base and agent in 10:1 weight ratio were manually stirred for 10 minutes and placed in a desiccator for 1 hour (Thermo Fisher Scientific, Waltham, MA) to remove air bubbles trapped in the mixture of PDMS. The degassed PDMS mixture was then poured into a mold 3D-printed by SLA printer (Photon S, ANYCUBIC, Hongkong) (Figure 3-a). The PDMS in a mold was placed on a 80 ℃ hotplate (SUPER-NUOVA, Thermo Fisher Scientific, Waltham, MA) for 1 hour for curing. Surface of the fully-cured PDMS was then treated with oxygen (O_2) plasma (75 W, 300 mTorr, 30 sccm O_2) for 10 seconds by a reactive ion etcher (RIE) (Sirius-T2, Trion Technology, Tempe, AZ) to enhance bonding

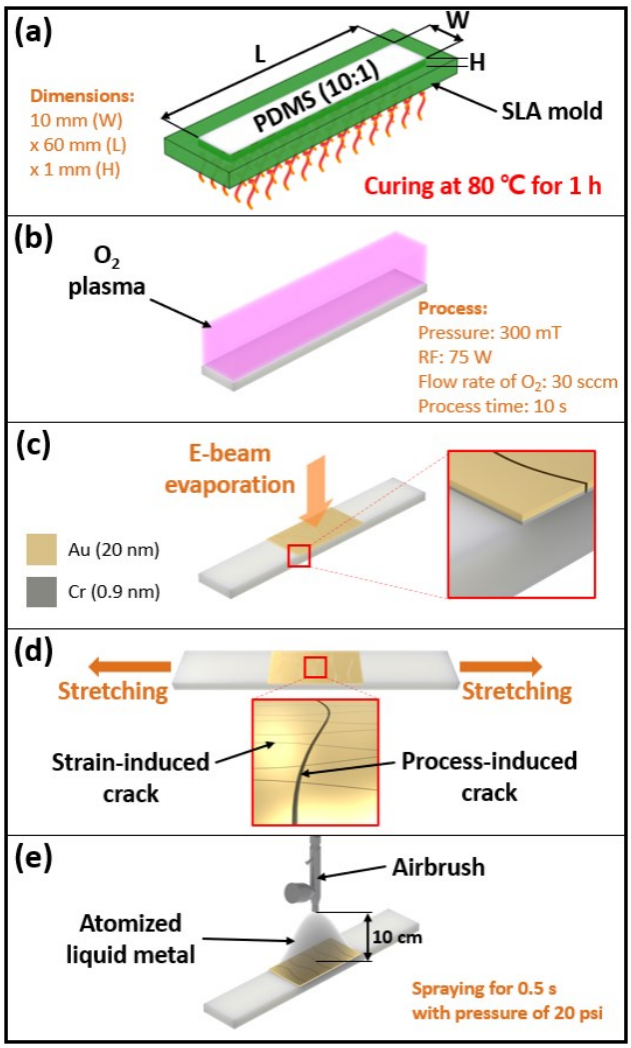

Fig. 3. Conceptual schematic diagrams of the fabrication process of the crack-based sensor decorated with atomized liquid metal droplets: (a) fabrication of a rectangular-shape PDMS as a body of crack-based sensor; (b) O_2 plasma treatment for enhanced bonding between the PDMS and the bilayer metal film; (c) deposition of Cr/Au metal bilayers using e-beam evaporation and naturally formed process-induced cracks; (d) formation of strain-induced cracks; (e) spray coating of atomized liquid metal droplets on the crack-based sensor using an airbrush.

between the surface of PDMS and metal layers (Figure 3-b). When the surface of PDMS is exposed to oxygen plasma for enhancement of bonding between metal layers and PDMS, the surface of PDMS is oxidized and it builds tensile residual stress on the surface of the PDMS (Figure 4-a). Next, chromium (Cr) and gold (Au) thin metal layers were deposited with the thickness of 0.9 nm and 20 nm, respectively using e-beam evaporator (BJD-1800, Ferrotec, Inc., Santa Clara, CA) (Figure 3-c). When metal films are deposited on top of the oxygen plasma-treated PDMS surface, metal film itself also builds tensile residual stress in it depending on the deposition rate of the metals (Figure 4-b). These combined residual tensile stresses in the bilayer metal films and the PDMS surface exceed ultimate tensile strengths of metal layers resulting in crack formation which is called the process-induced cracks (Figure 4-c). Size of the process-induced cracks varies depending on the dose of the oxygen plasma and thickness of the deposited metal bilayers [30, 31]. Various thickness combinations of the metal films were studied, and we found that when the thickness of Cr is larger than 1 nm for 20 nm Au, development of the process-induced cracks in the bilayer metals were significant and the metal was permanently disconnected even before applying any mechanical strain. Cr thickness of 0.9 nm was found to be optimal for 20 nm thick Au in creating process-induced cracks for high sensitivity.

Finally, liquid metal Galinstan (Changsha Rich Nonferrous Metals Co., Ltd., Hunan, China) was spray coated on the cracked metal films of the crack-based sensor using an airbrush (TG TALON, Paasche, Kenoshua, WI) (Figure 3-e). Through the spray coating, atomized liquid metal droplets (typical size in the range of 10 ~ 20 μm) were randomly dispersed over the cracked thin metal films. Various pressures, with/without a metallic mesh, and varying distances between the airbrush and the sample were studied. A pressure of 20 psi, spray time of 0.5 second, and the airbrush placed 10 cm directly above the sample showed most reproducible results on the formation of atomized liquid metal droplets on the crack-based strain sensor.

After the formation of the process-induced cracks, the bilayer metal film on PDMS was stretched intentionally to create uniformly distributed strain-induced cracks all over the metal bilayers (Figure 3-d). With 60 mm in length, 5 mm axial stretching (strain of 8.33 %) was used to create strain-induced cracks. Figure 5 shows optical images of the process-induced cracks and the strain-induced cracks formed on the Cr/Au bilayer metal film (images taken using microscope INM100, Leica, Wetzlar, Hesse, Germany).

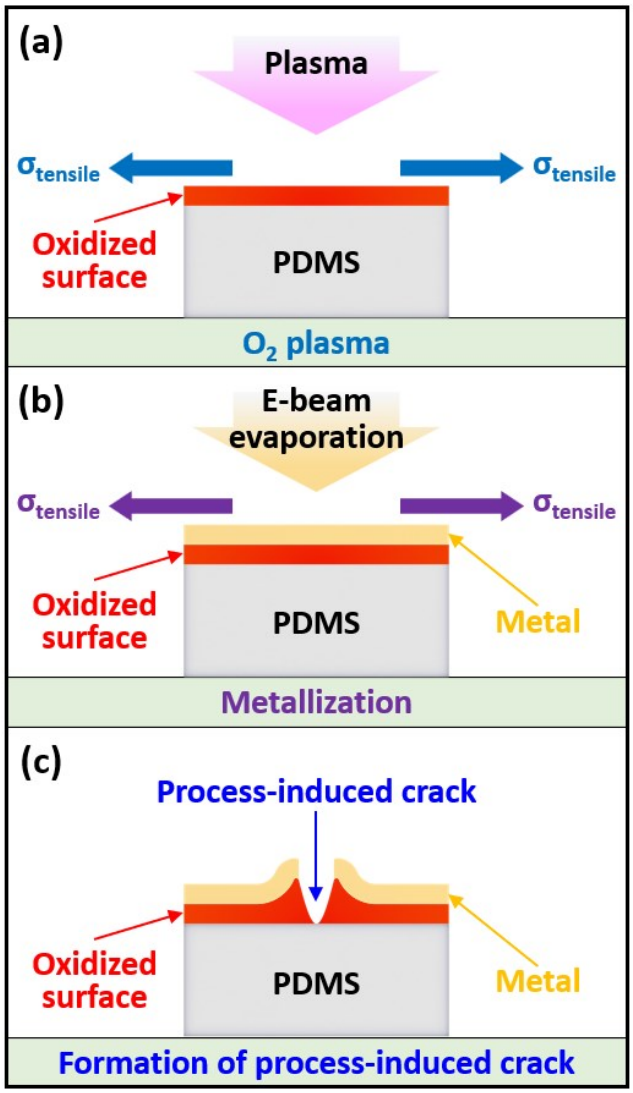

Fig. 4. Sequential schematic diagrams of formation of the process-induced crack: (a) tensile residual strain on the PDMS by oxygen (O_2) plasma exposure; (b) metal films-induced tensile residual strain; (c) formation of process-induced crack resulting from tensile residual strain.

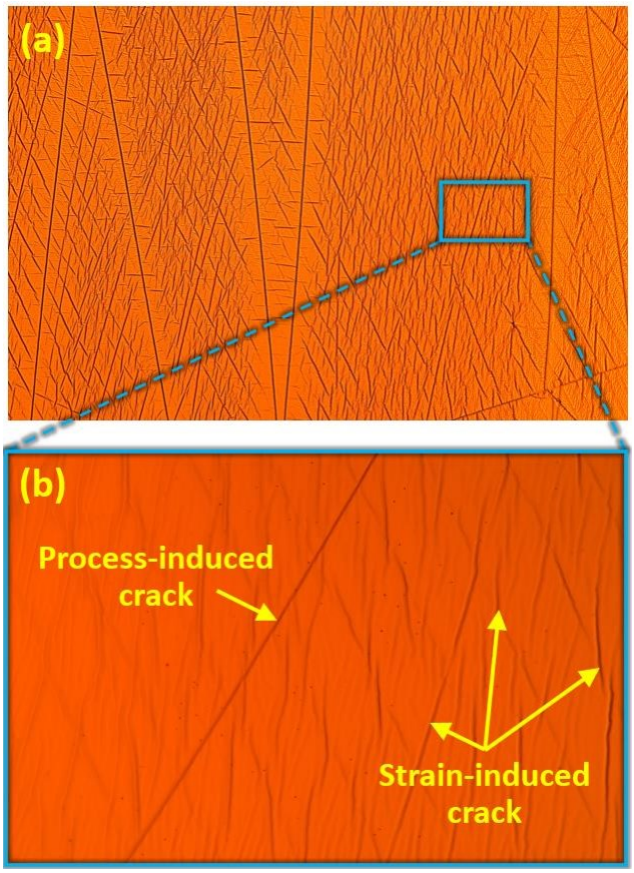

Fig. 5. Optical images of the process-induced cracks and the strain-induced cracks.

III. Experimental Results

A. Experimental setup

Figure 6 shows conceptual schematic diagram of the experimental setup for measuring the strain-induced resistance change in ultrasensitive crack-based sensor decorated with atomized liquid metal droplets. In order to apply tensile strain to the fabricated crack-based sensor, a load cell (Instron 6800 universal testing system, Norwood, MA) was utilized. A source measure unit (SMU) Keithley 2400 (Tektronix, Beaverton, OR) was used to measure change in resistance by measuring voltages with a current source. The measured data were acquired by LabVIEW (National Instruments, co., Austin, TX) program, and change in resistance as a function of applied axial strain were recorded.

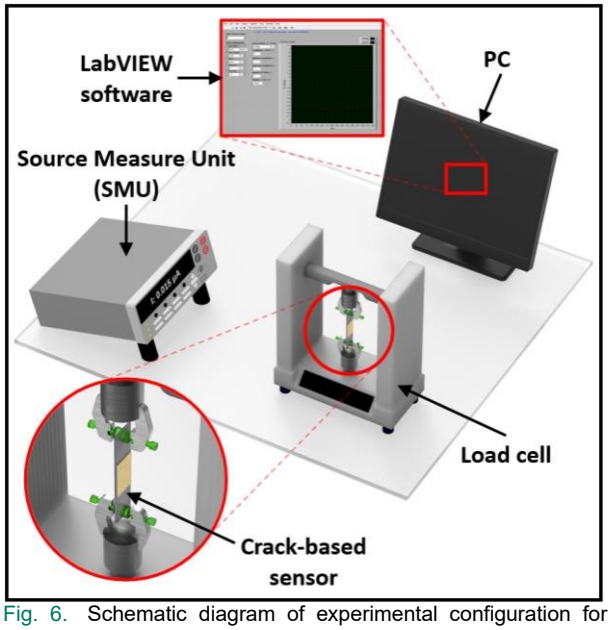

Fig. 6. Schematic diagram of experimental configuration for measuring a change in resistance of the crack-based sensors under a load cell.

B. Optical images of the crack-based sensor under the applied strain

Optical images of randomly dispersed atomized liquid metal droplets-decorated crack-based sensor under the applied axial strain are shown in Figure 7. In this sample, the crack-based sensor was not intentionally stretched before spray coating the liquid metal droplets to clearly show the development of strain-induced cracks. Figure 7-a1 shows surface of the strain sensor at initial state (applied strain of 0 %). The image shows randomly dispersed atomized liquid metal droplets all over the crack-based strain sensor. Figure 7-a2 shows a high magnification image of a liquid metal droplet sitting directly on a cracked line. With an axial mechanical strain of 5 %, the crack-based sensor stretched in the axial direction, and a lot of strain-induced cracks are developed (Figure 7-b1). From the captured snapshot, under the applied strain, atomized liquid metal droplet shows stretching in the axial direction due to the sticky characteristic of oxide skin of the liquid metal. When an axial mechanical strain of 10 % was applied, there was huge increase in strain-induced cracks while the liquid metal droplet still connects the metal films above the cracks.

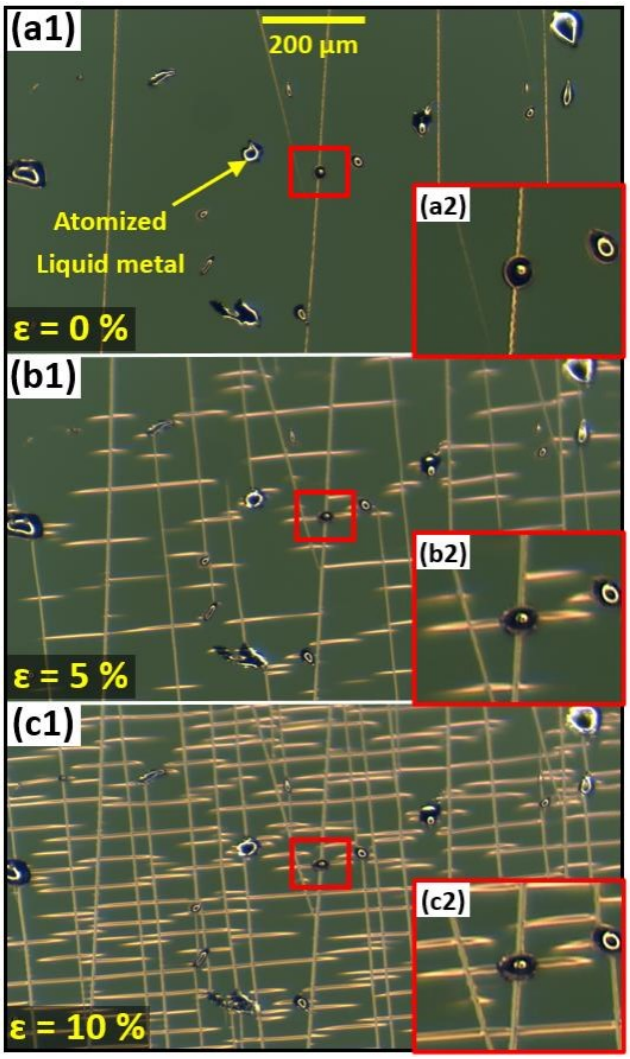

Fig. 7. Optical images of ultrasensitive crack-based sensor decorated with randomly-dispersed atomized liquid metal droplets from top view under the strain of (a) 0% (initial state), (b) 5%, and (c) 10%.

C. Measurement results

Figure 8 shows measurement results of the crack-based strain sensors with and without liquid metal droplet decoration. The first sample was one with bilayer Cr/Au metal layers on PDMS (green) without liquid metal and the second sample was with randomly dispersed atomized liquid metal droplets decorated over the bilayer Cr/Au metal films on PDMS (orange). In the case of the crack-based sensor without atomized liquid metal droplets, as expected, ultrahigh sensitivity (R/R_0) of ~39 was obtained near the maximum axial strain of 2 % which yields a gauge factor of 1,713. However, the sensor was not functioning beyond the axial strain of 2.283 % as the bilayer metal film was completely disconnected.

The crack-based sensor decorated with atomized liquid metal droplets showed lower sensitivity compared to the crack-based sensor without liquid metal in the region of low applied axial

strain (0~2 %). However, the sensor with the liquid metal was continually operational well beyond the sensing range limit of the sensor without liquid metal (2.283%). The sample showed very high sensitivity in the sensing range of 6~10% with a gauge factor of > 2,000. The sensor with liquid metal finally completely disconnected when an axial mechanical strain goes beyond 10.675 %. This is a substantial improvement in sensing range (by a factor of 4.7) compared to that of the sensor without liquid metal. At the applied strain of 10.675%, maximum sensitivity (R/R_0) of ~238 was achieved yielding gauge factor of ~2,230.

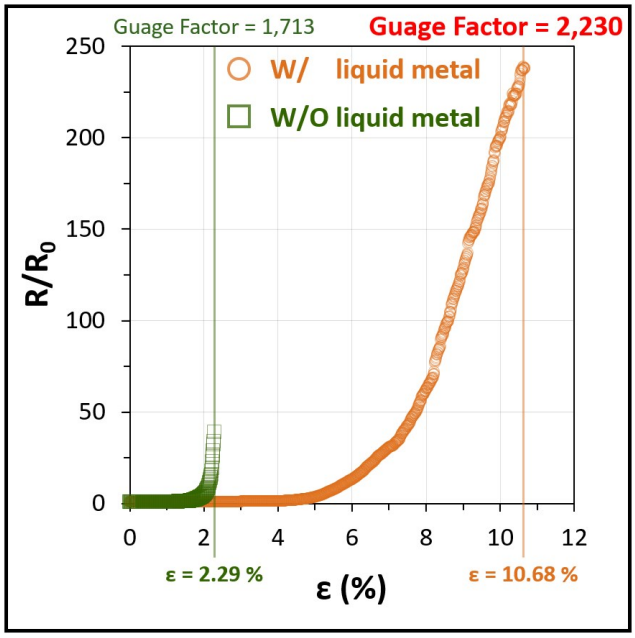

Fig. 8. Normalized resistance as a function of the axial strain for the crack-based sensor without liquid metal and the sensor decorated with randomly dispersed atomized liquid metal droplets.

Table 1 shows comparison of sensitivity and sensing range of our crack-based sensors with previously reported crack-based sensors.

TABLE I
COMPARISON OF SENSITIVITY AND SENSING RANGE IN OUR WORK WITH OTHER CRACK-BASED SENSORS

Reference	Sensitivity (R/R_0)	Sensing Range (%)
[21]	34	0-2
[32]	45	0-2
[33]	45	0-2
[34]	160	0-1.5
[35]	34	0-2
[36]	16	0-2.2
[37]	300	0-2
[38]	520	0-2
[39]	66	0-2
[40]	9	0-0.025
Our work without liquid metal	39	0-2.28
Our work with liquid metal	238	0-10.68

D. Flexibility and stability of the crack-based sensor

Since the crack-based sensor proposed here is fabricated by liquid metal decoration on cracked thin bilayer metal film on PDMS, the sensor is physically flexible. We tested the physical flexibility of the sensor by stretching, bending, and twisting. Figure 9 shows optical images of flexibility demonstration of the fabricated crack-based sensor with liquid metal decoration. Regardless of repeated motions, atomized liquid metal droplets were not detached from the crack-based sensor.

To test the sensor's stability, we did a cyclic loading of a total of 200 cycles of stretching/releasing with the strain in the range of 0~10%. Figure 10 shows sensitivity of the liquid metal decorated crack-based sensor during 200 cyclic loading. There was no apparent irregularity in the sensitivity during this cyclic loading test, nor any apparent visually noticeable damage on the sensor.

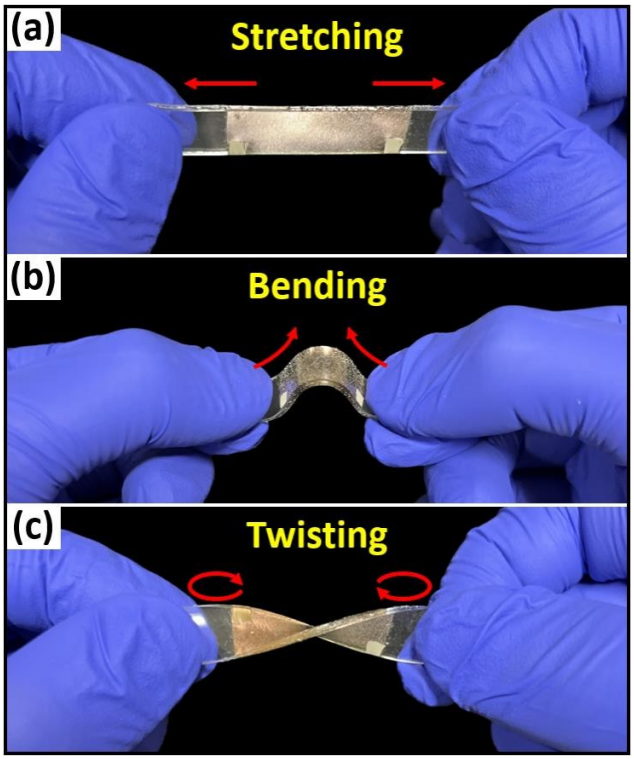

Fig. 9. Optical images of flexibility test for crack-based sensor decorated with randomly dispersed atomized liquid metal droplets under various motions of (a) stretching, (b) bending, and (c) twisting.

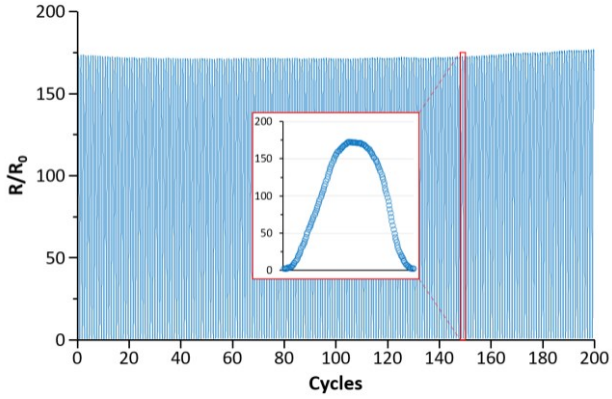

Fig. 10. Sensitivity of the crack-based sensor decorated with atomized liquid metal droplets during 200 cycles of stretching/releasing with the strain of 0~10 %.

IV. Conclusion

Random dispersion of atomized liquid metal droplets on the crack-based sensor was proposed as a method of enhancing the sensing range and stability of the sensor. The proposed method of fabrication of the sensor is extremely simple, but nearly 5x sensing range enhancement along with a slight increase in sensitivity with increased stability were achieved due primarily to sticky and extendable nature of oxidized liquid metal droplets. The fabricated sensor is physically flexible (bendable, foldable, stretchable) and extended cyclic loading test showed no apparent damage on the sensor. This research outcome may be greatly helpful for developing ultrasensitive wearable strain sensors with high stability in practical applications.

Acknowledgment

This work was supported in part by the United States National Science Foundation grant NSF ECCS–1908779. The authors would like to acknowledge Dr. Hongbing Lu and his Lab member at UT Dallas for technical assistance. We also would like thank Mohammad Salman Parvez, Muhammad Luqman Haider, Tanzila Noushin and UT Dallas Clean Room staff for their support.

References

[1] S. K. Ghosh, P. Adhikary, S. Jana, A. Biswas, V. Sencadas, S. D. Gupta, B. Tudu, and D. Mandal, "Electrospun gelatin nanofiber based self-powered bio-e-skin for health care monitoring," Nano Energy, vol. 36, pp. 155-175, Jun. 2017.

[2] A. Green, and J. Kirk," Guidelines for the performance of the sweat test for the diagnosis of cystic fibrosis," Ann. Clin. Biochem., vol. 44, no. 1, pp. 25-34, Jan. 2007.

[3] M. A. Shahbazi, N. Shrestha, M. K. Pierchala, F. B. Kadumudi, M. Mehrali, M. Hasany, V. Préat, S. Leeuwenburgh, and A. Dolatshahi-Pirouz, "A self-healable, moldable and bioactive biomaterial gum for personalised and wearable drug delivery," J. Mater. Chem., vol. 8, no. 19, pp. 4340-4356, May 2020.

[4] W. Qi, and H. Su, "A cybertwin based multimodal network for ecg patterns monitoring using deep learning," IEEE T. In. Inform., vol. 18, no. 10, pp. 6663-6670, Mar. 2022.

[5] S. Nakata, T. Arie, S. Akita, and K. Takei, "Wearable, flexible, and multifunctional healthcare device with an ISFET chemical sensor for simultaneous sweat pH and skin temperature monitoring," ACS Sens., vol. 2, no. 3, pp. 443-448, Mar. 2017.

[6] J. W. Lee, D. C. Han, H. J. Shin, S. H. Yeom, B. K. Ju, and W. Lee, "PEDOT: PSS-based temperature-detection thread for wearable devices," Sensors, vol. 18, no. 9, pp. 2996, Sep. 2018.

[7] S. Ryu, P. Lee, J. B. Chou, R. Xu, R. Zhao, A. J. Hart, and S. G. Kim," Extremely elastic wearable carbon nanotube fiber strain sensor for monitoring of human motion," ACS nano, vol. 9, no. 6, pp. 5929-5936, Jun. 2015.

[8] Y. Wang, L. Wang, T. Yang, X. Li, X. Zang, M. Zhu, K. Wang, D. Wu, and H. Zhu, " Wearable and highly sensitive graphene strain sensors for human motion monitoring," Adv. Funct. Mater., vol. 24, no. 29, pp. 4666-4670, Aug. 2014.

[9] N. Afsarimanesh, S. C. Mukhopadhyay, and M. Kruger, "Molecularly imprinted polymer-based electrochemical biosensor for bone loss detection," IEEE T. Bio-med. Eng., vol. 65, no. 6, pp. 1264-1271, Aug. 2017.

[10] N. Afsarimanesh, M. E. Alahi, S. C. Mukhopadhyay, and M. Kruger, "Development of IoT-based impedometric biosensor for point-of-care monitoring of bone loss," IEEE J. Em. Sel. Top. C., vol. 8, no. 2, pp. 211-220, Mar. 2018.

[11] S. Chen, J. Qi, S. Fan, Z. Qio, J. C. Yeo, and C. T. Lim, "Flexible wearable sensors for cardiovascular health monitoring," Adv. Healthc. Mater., vol. 10, no. 17, pp. 2100116, Sep. 2021.

[12] S. Kang, V. P. Rachim, J. H. Baek, S. Y. Lee, and S. M. Park, "A flexible patch-type strain sensor based on polyaniline for continuous monitoring of pulse waves," IEEE Access, vol. 8, pp. 152105-152115, Aug. 2020.

[13] B. Park, S. Lee, H. Choi, J. U. Kim, H. Hong, C. Jeong, D. Kang, and T. I. Kim, "A semi-permanent and durable nanoscale-crack-based sensor by on-demand healing," Nanoscale, vol. 6, no. 2, pp. 38, Apr. 2021.

[14] S. Y. Cho, H. Yu, J. Choi, H. Kang, S. Park, J. S. Jang, H. J. Hong, I. D. Kim, S. K. Lee, H. S. Jeong, and H. T. Jung, "Continuous meter-scale synthesis of weavable tunicate cellulose/carbon nanotube fibers for high-performance wearable sensors," ACS nano, vol. 13, no. 8, pp. 9332-9341, Aug. 2019.

[15] S. Roy, M. David-Pur, and Y. Hanein, "Carbon nanotube-based ion selective sensors for wearable applications," ACS Appl. Mater. Inter., vol. 9, no. 40, pp. 35169-35177, Oct. 2017.

[16] S. Ryu, P. Lee, J. B. Chou, R. Xu, R. Zhao, A. J. Hart, and S. G. Kim, "Extremely elastic wearable carbon nanotube fiber strain sensor for monitoring of human motion," ACS Nano, vol. 9, no. 6, pp. 5929-5936, Jun. 2015.

[17] J. Bujes-Garrido, D. Izquierdo-Bote, A. Heras, A. Colina, and M. J. Acros-Martinez, "Determination of halides using Ag nanoparticles-modified disposable electrodes. A first approach to a wearable sensor for quantification of chloride ions," Anal. Chim. Acta, vol. 1012, pp. 42-48, Jul. 2018.

[18] K. Y. Ko, L. T. Huang, and K. J. Lin, "Green technique solvent-free fabrication of silver nanoparticle–carbon nanotube flexible films for wearable sensors," Sensor Actuat. A-Phys., vol. 317, pp. 112437, Jan. 2021.

[19] S. M. Doshi, C. Murray, A. Chaudhari, D. H. Sung, and E. T. Thostenson, "Ultrahigh sensitivity wearable sensors enabled by electrophoretic deposition of carbon nanostructured composites onto everyday fabrics," J. Mater. Chem., vol. 10, no. 5, pp. 1617-1624, Jan. 2022.

[20] A. N. Kozitsina, T. S. Svalova, N. N. Malysheva, A. V. Okhokhonin, M. B. Vidrevich, and K. Z. Brainina, "Sensors based on bio and biomimetic receptors in medical diagnostic, environment, and food analysis," Biosensors, vol. 8, no. 2, pp. 35, Jun. 2018.

[21] D. Kang, P. V. Pikhitsa, Y. W. Choi, C. Lee, S. S. Shin, L. Piao, B. Park, K. Y. Suh, T. I. Kim, and M. Choi, "Ultrasensitive mechanical crack-based sensor inspired by the spider sensory system," *Nature*, vol. 516, no. 7530, pp. 222-226, Dec. 2014.

[22] B. Park, J. Kim, D. Kang, C. Jeong, K. S. Kim, J. U. Kim, P. J. Yoo, and T. I. Kim, "Dramatically enhanced mechanosensitivity and signal-to-noise ratio of nanoscale crack-based sensors: effect of crack depth," *Adv. Mater.*, vol. 28, no. 37, pp. 8130-8137, Oct. 2016.

[23] Y. Zhou, P. Zhan, M. Ren, G. Zheng, K. Dai, L. Mi, C. Liu, and C. Shen, "Significant stretchability enhancement of a crack-based strain sensor combined with high sensitivity and superior durability for motion monitoring," *ACS Appl. Mater. Inter.*, vol. 11, no. 7, pp. 7405-7414, Jan. 2019.

[24] D. Kim, D. Jung, J. H. Yoo, Y. Lee, W. Choi, G. S. Lee, K. Yoo, and J. B. Lee, "Stretchable and bendable carbon nanotube on PDMS super-lyophobic sheet for liquid metal manipulation," *J. Micromech. Microeng.*, vol. 24, no. 5, pp. 055018, Apr. 2014.

[25] D. Kim, R. G. Pierce, R. Henderson, S. J. Doo, K. Yoo, and J. B. Lee, "Liquid metal actuation-based reversible frequency tunable monopole antenna," *Appl. Phys. Lett.*, vol. 105, no. 23, pp. 234104, Dec. 2014.

[26] J. Jeong, J. B. Lee, S. K. Chung, and D. Kim, "Electromagnetic three dimensional liquid metal manipulation," *Lab Chip*, vol. 19, no. 19, pp. 3261-3267, Aug. 2019.

[27] D. Kim, P. Thissen, G. Viner, D. W. Lee, W. Choi, Y. J. Chabal, and J. B. Lee, "Recovery of nonwetting characteristics by surface modification of gallium-based liquid metal droplets using hydrochloric acid vapor," *ACS Appl. Mater. Inter.*, vol. 5, no. 1, pp. 179-185, Jan. 2013.

[28] D. Kim, Y. Lee, D. W. Lee, W. Choi, K. Yoo, and J. B. Lee, "Hydrochloric acid-impregnated paper for gallium-based liquid metal microfluidics," *Sensor Actuat. B-Chem.*, vol. 207, pp. 199-205, Feb. 2015.

[29] B. Feng, X. Jiang, G. Zou, W. Wang, T. Sun, H. Yang, G. Zhao, M. Dong, Y. Xiao, H. Zhu, and L. Liu, "Nacre-Inspired, Liquid Metal-Based Ultrasensitive Electronic Skin by Spatially Regulated Cracking Strategy," *Adv. Funct. Mater.*, vol. 31, no. 29, pp. 2102359, Jul. 2021.

[30] R. Seghir, and S. Arscott, "Controlled mud-crack patterning and self-organized cracking of polydimethylsiloxane elastomer surfaces," Sci. Rep., vol. 5, no. 1, pp. 14787, Oct. 2015.

[31] T. Baětens, E. Pallecchi, V. Thomy, and S. Arscott, "Cracking effects in squashable and stretchable thin metal films on PDMS for flexible microsystems and electronics," *Sci. Rep.*, vol. 8, no. 1, pp. 1-17, Jul. 2018.
[32] B. Park, J. U. Kim, J. Kim, D. Tahk, C. Jeong, J. Ok, J. H. Shin, D. Kang, and T. I. Kim, "Strain-visualization with ultrasensitive nanoscale crack-based sensor assembled with hierarchical thermochromic membrane," Adv. Funct. Mater., vol. 29, no. 40, pp. 1903360, Oct. 2019.
[33] B. Park, S. Lee, H, Choi, J. U. Kim, H. Hong, C. Jeong, D. Kang, and T. I. Kim, "A semi-permanent and durable nanoscale-crack-based sensor by on-demand healing." Nanoscale, vol. 10, no. 9, pp. 4354-4360, Jan. 2018.
[34] T. Kim, I. Hong, M. Kim, S. Im, Y. Roh, C. Kim, J. Lim, D. Kim, J. Park, S. Lee, and D. Lim, "Ultra-stable and tough bioinspired crack-based tactile sensor for small legged robots," npj Flex., vol. 7, no. 1, pp. 22, Apr. 2023.
[35] T. Lee, Y. W. Choi, G. Lee, S. M. Kim, D. Kang, and M. Choi, "Crack-based strain sensor with diverse metal films by inserting an inter-layer," RSC Adv., vol. 7, no. 55, pp. 34810-34815, July 2017.
[36] S. Chen, Y. Wei, S. Wei, Y. Lin, and L. Liu, "Ultrasensitive cracking-assisted strain sensors based on silver nanowires/graphene hybrid particles," ACS Appl. Mater. Inter., vol. 8, no. 38, pp. 25563-25570, Sep. 2016.
[37] R. Madhavan, "Network crack-based high performance stretchable strain sensors for human activity and healthcare monitoring," New J. Chem., vol. 46, no. 36, pp. 17596-17609, Aug. 2022.
[38] T. Kim, T. Lee, G. Lee, Y. W. Choi, S. M. Kim, D. Kang, and M. Choi, "Polyimide encapsulation of spider-inspired crack-based sensors for durability improvement," Appl., vol. 8, no. 3, pp. 367, Mar. 2018.
[39] M. Kim, H. Choi, T. Kim, I. Hong, Y. Roh, J. Park, S. Seo, S. Han, J. S. Koh, and D. Kang, "FEP encapsulated crack-based sensor for measurement in moisture-laden environment," Mater., vol. 12, no. 9, pp. 1516, May 2019.
[40] N. D. P. Ferreira, E. Puyoo, B. Massot, S. Brottet, and C. Malhaire, "Portable device integrating an ultrasensitive mechanical crack-based sensor for the wireless monitoring of cardiac activity," 2020 Symposium on Design, Test, Integration & Packaging on MEMS and MOEMS (DTIP), IEEE, pp. 1-5, Jun. 2020.

Jinwon Jeong (Graduate Student Member, IEEE) received the B.S. and M.S. degrees in Mechanical Engineering from Myongji University, Yongin, South Korea, in 2018 and 2020, respectively. He is currently pursuing Ph.D. degree in the Department of Electrical and Computer Engineering at The University of Texas at Dallas, Richardson, TX, USA. His current research interests include MEMS, liquid metal, reverse electrowetting on dielectric (REWOD), and microrobot.

Arkadeep Mitra (Graduate Student Member, IEEE) received his B.Tech in Electrical Engineering from KIIT University, Bhubaneswar, India in 2013 and his MSEE degree specializing in Nanotechnology and MEMS – Materials and Devices from the University of Texas at Arlington in 2017. He worked as a software engineer in Aricent, Gurgaon during 2013-2015. He completed his Ph.D. in Electrical Engineering from the University of Texas at Dallas (UTD) in 2022. He is now working for Lam Research (Fremont, CA).

Jeong Bong (JB) Lee (Senior Member, IEEE) received the B.S. degree in Electronics Engineering from Hanyang University, Seoul, South Korea, in 1986, and the M.S. and the Ph.D. degrees in Electrical Engineering from Georgia Institute of Technology, Atlanta, GA, USA, in 1993 and 1997, respectively. He joined The University of Texas at Dallas in May 2001, after two and a half years at the Louisiana State University as an assistant professor. He is a full professor and an associate department head for the graduate programs. His current research interests include MEMS, sensors, biomedical devices, and liquid metal. Dr. Lee was a recipient of the National Science Foundation CAREER Award in 2001.He serves as a Technical Program Committee (TPC) Co-Chair for the IEEE Sensors 2023 Conference and will serve as the General Chair of the ISOEN (International Symposium on Olfaction and Electronic Nose) 2024. He also serves as an associate editor for the IEEE Sensors Journal. He has served as a TPC co-chair for the IEEE Sensors 2022 Conference, an Editorial Board Member for several other journals, an Executive TPC member for Transducers along with other services.